PROC. OF JSCE,
No. 312, August 1981

INITIATION AND PROPAGATION OF FATIGUE CRACKS IN PARTIALLY-PENETRATED LONGITUDINAL WELDS

By Chitoshi MIKI, Fumio NISHINO***
*Jiro TAJIMA*** and Yoshitaka KISHIMOTO****

1. INTRODUCTION

Conventionally, evaluations of safety against fatigue of structures have been made based on S-N diagrams obtained in fatigue tests of structural members and specimens of joint portions. Current fatigue designs of bridges also are made using allowable stresses set up taking into account suitable safety factors on fatigue limits (in most cases 2×10^6-cycles strength) obtained from such fatigue tests[1]. Such a method is direct, and reliability is assured to some extent. However, even though structural members and joints themselves are tested, the configurations and dimensions of specimens are subject to considerable restrictions because of limitations to capabilities of testing machines, and thorough care must be exercised in the application of the results.

Fatigue failure is a phenomenon which can be subdivided into initiation of fatigue crack and propagation of the crack up to failure of the member. Initiation of fatigue crack is a localized phenomenon which occurs at a location in the member where stress conditions are unfavorable, and the life up to that time (crack initiation life: N_c) is greatly influenced by localized stress concentrations and weld defects in the member. In contrast, the life up to failure of the member upon propagation of fatigue crack (crack propagation life: N_p) varies depending on the dimensions of the member and overall stress distribution. In case of being subject to variable stresses fluctuations such as actual stresses by vehicle, it is possible to estimate N_c applying the linear damage law, but the application is difficult for N_p[2]. Accordingly, it is thought that fatigue safety of a structure should be evaluated distinguishing between N_c and N_p.

Various definitions may be given N_c depending on the dimensions of the fatigue crack used as the basis, but it is practical to define N_c as the number of cycles of stressing until occurrence of a macroscopic fatigue crack of dimensions of the degree that it could be taken up as a subject in fracture mechanics. This is thought to correspond to the time when the propagation mechanism of fatigue cracking has entered its second stage[3]. The fatigue crack propagation life can be estimated by fracture mechanics techniques using the stress intensity factor and the fatigue crack growth rate, and applications to various joint portions have been attempted[4)~8)]. In such cases, it is necessary to assume the configurations and dimensions of the initial crack, the configurations of cracks during propagation, and the final configurations and dimensions of cracks, and therefore, having a grasp of the initiation of fatigue crack at actual joint portions and subsequent conditions of propagation will be most fundamental for application of fracture mechanics.

In the present study, examinations are made of partially-penetrated single-bevel groove joints used for corner welds of box-section truss members. The authors have already clarified the great influence of residual welding stress on the fatigue strength of a joint, and that fatigue crack is initiated with the portion of irregularity at the root of the weld as the starting point[9]. However, the initiation of fatigue crack and the conditions of propagation had not been adequately grasped.

In order to confirm the initiation and propagation of a fatigue crack, ① the surface of the specimen may be directly inspected with a magnifying glass or microscope, ② a sample may be collected from the surface of the specimen and inspected by microscope, ③ ultrasonic waves may be employed, ④ marking may be done with

* Dr. Eng., Associate Professor, of Dept., Civil Engineering, University of Tokyo.
** Ph. D., Professor, Dept., of Civil Engineering, University of Tokyo.
*** Dr. Eng., Professor, Dept., of Construction Engineering, Saitama University.
**** M. Eng., 2nd Design Dept., Honshu-Shikoku Bridge Aouthority.

a dye of good penetration properties, or ⑤ beach marks may be left on fracture surfaces. Of these, ① and ② are difficult to implement except when fatigue cracks are initiated in small limited areas at the surfaces of specimens, measurements of configurations and dimensions of fatigue cracks cannot be made with ③, while ④ is effective only when fatigue cracks are initiated at the surface and propagation of the cracks cannot be observed. In case of the partially-penetrated longitudinal welds taken up in this paper, since fatigue cracks are initiated at the interiors of plates, while it was desired to clarify the propagation properties of the fatigue cracks, the method of ⑤ was adopted. Beach marks are striae left on the fracture surface when stress conditions change after a fatigue crack has been initiated, and are due to variations in the fatigue crack growth rate. Consequently, by varying the loading amplitude at every given number of cycles and companying the loading history and number of beach marks after testing, it will be possible to obtain the approximate number of cycles at which the fatigue crack was initiated, while the variation in the configuration of the fatigue crack accompanying propagation of the crack will be clarified from the configurations of the beach marks, and the fatigue crack growth rate from the spacings between beach marks.

2. METHOD OF TESTING

(1) Specimens

The specimens used in this study were made of 800 N/mm² class quenched and tempered high tension steel, the mechanical properties and chemical composition of which are shown in **Table 1**.

Test plates, after their four sides were welded to restricting plates of thickness of 50 mm, were welded at longitudinal grooves. This was done with the objectives of introducing high residual stresses at longitudinal welds, preventing welding deformation, and maintaining the restrained conditions of all specimens constant. Grooves were machined, while welding was done manually by a single skilled welder. The mechanical properties and chemical composition of the electrodes used are shown in **Table 2** and the welding condition records in **Table 3**. With the purpose of making the configurations of roots of

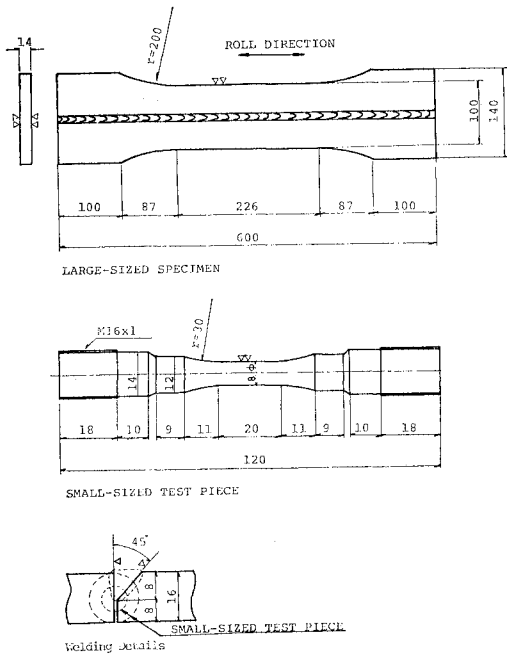

Fig. 1 Specimen Configurations and Dimensions.

Table 1 Mechanical Properties and Chemical Composition of Steels in Test (Mill Sheet Values).

Mechanical Properties			Chemical Composition									
σ_Y kg/mm² (N/mm²)	σ_U kg/mm² (N/mm²)	*El* (%)	C ×100	Si ×100	Mn ×100	P ×1 000	S ×1 000	Cu ×100	Cr ×100	Mo ×100	V ×100	B ×10 000
84 (823)	87 (853)	33	11	25	88	15	5	26	76	40	4	8

Table 2 Mechanical Properties and Chemical Composition of Electrodes (Mill Sheet Values).

	Mechanical Properties			Chemical Composition (Weld Metal)							
Size	σ_Y kg/mm² (N/mm²)	σ_U kg/mm² (N/mm²)	*El* (%)	C ×100	Mn ×100	Si ×100	P ×1 000	S ×1 000	Ni ×100	Cr ×100	Mo ×100
4*	75.1 (736)	84.2 (825)	24	7	142	60	11	6	184	30	42
5**	77.2 (757)	85.9 (842)	22	7	160	70	16	7	186	29	41

* Used for First Pass.
** Used for Second Pass.

Table 3 Welding Condition Records of Specimens.

Pass	Preheating Temperature (C)	Electric Current (A)	Heat Input J/cm
1	150	160	16 000—19 000
2	150	240	21 000—24 000

welds where fatigue cracks would be initiated to be about the same, stops and restarts were made at locations to be the centers of specimens of all test plates. The root gap of all specimens was 0 mm.

The configurations and dimensions of specimens finished from the test plates are as shown in **Fig. 1**, these consisting of plate specimens having parallel portions of 100-mm widths and round rod test pieces cut out from welds including root portions (hereafter called large-sized specimens and small-sized test pieces, respectively).

(2) Performance of Fatigue Tests

Fatigue tests of large-sized specimens and small-sized test pieces were performed using hydraulic survo-controlled fatigue testing machines having dynamic capacities of ± 50 tons for the former and ± 5 tons for the latter. The load waveform was that of sine waves, and the loading frequency was 10 Hz.

Fatigue tests of large-sized specimens were performed with pulsating loads of minimum stress of approximately 10 N/mm^2 and with completely alternating loads. All small-sized test pieces were subjected to pulsating load fatigue tests of minimum stress of approximately 10 N/mm^2.

The fatigue tests performed, besides constant stress range tests, included also two-stage multi-stress amplitude tests (beach mark tests) where stress range was decreased to one half every certain number of cycles with the purpose of leaving beach marks on fracture surface. In this study, the number of cycles in large amplitude step and small amplitude step is equal. The number of cycles in one block was 3×10^4 to 1×10^5 cycles. A scaled microscope ($10x$—$46x$) was used for measuring sizes of beach marks. The accuracy of measuring was about 0.01 mm.

(3) Measurement of Residual Welding Stress

Residual welding stress was obtained by pasting a strain gage on the cross section of the specimen to be measured and measuring the strain relieved when a small piece of 10 mm × 10 mm was cut out with a saw. The gages used were triaxial gages of gage length of 2 mm (KFC-2-D17-11: Kyowa Electronic Instruments).

Measurements were made only on specimens for which fatigue tests had been finished. This was because residual welding stresses are sometimes redistributed at the first cycle of fatigue tests and subsequent changes are small, and because it is the residual stress after redistribution which is concerned with fatigue strength[9]. The cross sections for measurements of the various specimens were the parallel sections more than 100 mm distant from failure locations[9].

3. RESULTS OF CONSTANT STRESS RANGE FATIGUE TESTS

(1) S-N_f Curve Diagram

The results of constant stress range fatigue tests with stress range (S) taken on the ordinate and number of cycles until failure (N_f) on the abscissa, both on logarithmic scale, give the S-N_f diagram of **Fig. 2**. The straight line in the diagram was obtained by the method of

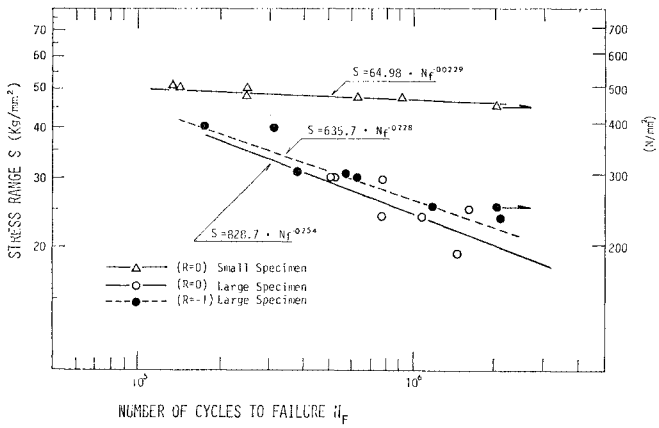

Fig. 2 Results of Constant Stress Range Fatigue Tests.

least squares.

There were practically no differences in fatigue strengths between alternating stress conditions and pulsating stress conditions. This was due to high residual tensile stresses existing at welds where fatigue cracks were initiated. As stated in the previous report[9], there was a large difference between the fatigue strengths of small-sized test pieces and large-sized specimens, and it is clear that reduction in fatigue strength due to the existence or residual welding stress is very great.

(2) Residual Welding Stress Distribution

The results of measurements of residual welding stresses are shown in **Fig. 3**. These were specimens for which fatigue tests had been finished and the axial-direction residual stresses (σ_x) were very high tensile stresses at the welds and their vicinities. The residual stresses (σ_y) in the direction perpendicular to the axis were very small and were values close to zero at the weld metal.

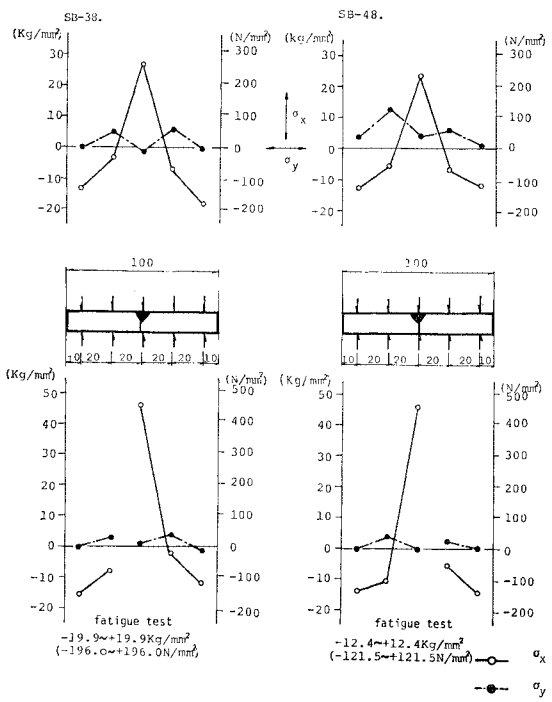

Fig. 3 Residual Welding Stress Distributions.

(3) Penetration Condition of Weld Metal and Initiation of Fatigue Cracks

With the purpose of investigating the relation between the condition of penetration of weld metal at roots of welds and the locations of fatigue crack initiation, all large-sized specimens after fatigue tests were ruptured along weld lines and the fracture planes were observed. Since rupturing was done after thoroughly chilling with liquid nitrogen, plastic deformation was not produced at fracture planes.

Photo 1 is an example of a fracture plane obtained in such manner. In all of the specimens, the penetration of weld into groove was insufficient, and there are unfused portions of height of 1 to 2 mm in tunnel form left remaining along the entire lengths of the welds. Judging by studies in the past[9,11], given the conditions of root gap of 0 mm for a 45-degree single-bevel groove and manual welding, it is unavoidable for such unfused portions to remain. At the locations where stopping and restarting were done, there were fairly large irregularities formed at the bottom surfaces of welds, while irregular rises and falls were produced at other parts. Fatigue cracks were initiated from locations where configuration changes of bottom surfaces of welds were large such as in the case of the above, or in the case of initiation from the depressed parts of ripples formed at the surface where the configuration changes were small but acute. Specimen SB-45 in **Photo 1** was ruptured on propagation of a fatigue crack from the stop and restart location, but there were two other places where fatigue cracks were formed. The failures of Specimens SB-44 and SB-46 were caused by fatigue cracks initiated from points other than stop and restart locations, but fatigue cracks formed from stop and restart locations also had reached the surfaces of the specimens. The occurrences of fatigue cracks from stop and restart locations, and the formation of a plural number of fatigue cracks at the parallel portions of specimens are phenomena in common for almost all of the specimens.

4. RESULTS OF BEACH MARK TESTS

(1) Observation of Beach Marks

Photo 2 shows an example of a fracture surface with beach marks, while **Fig. 4** indicates stress histories and the results of observations of beach marks of the test specimens. A beach mark, from its formation mechanism, expresses the configuration of fatigue cracking at the time of variation in stress conditions.

The specimen, SB-36, showed fatigue failure during the ninth halving of the stress range. From comparisons of beach marks and stress histories, the beach mark 1 was formed by the first reduction to half of the stress range, and with this specimen, it is clear that the fatigue crack had been initiated and propagation started

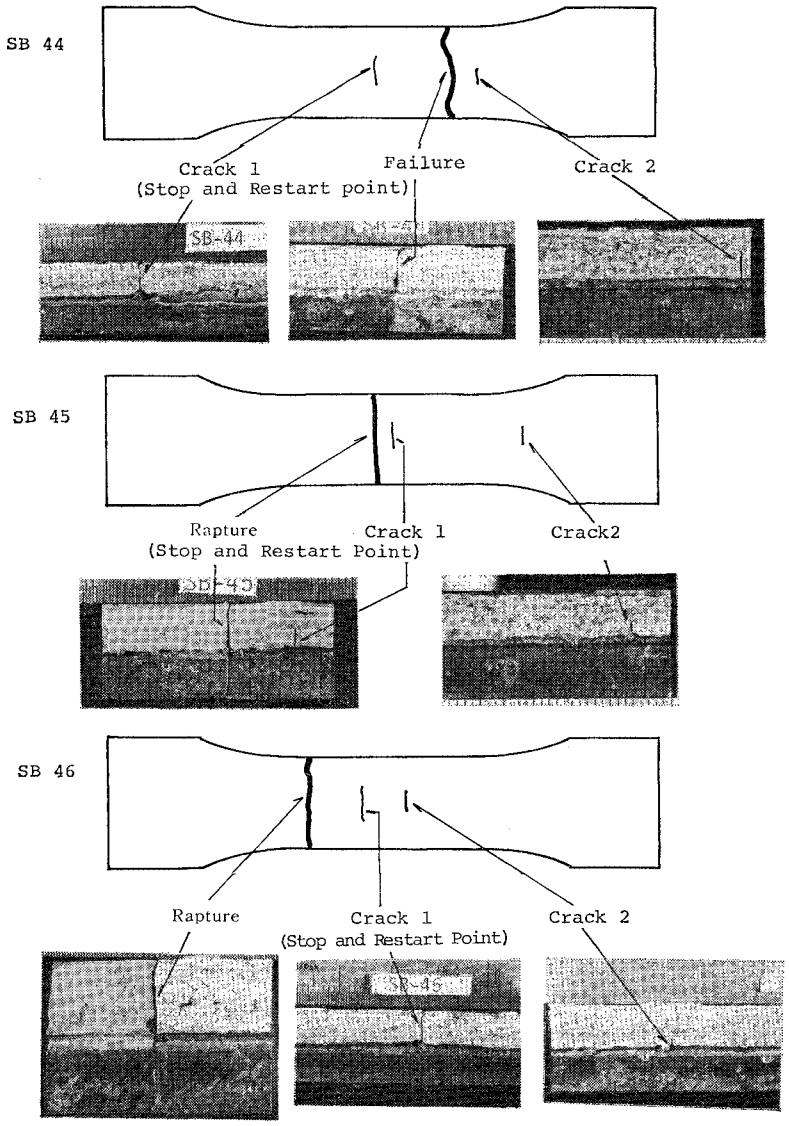

Photo 1 Configuration of Weld Metal at Root and Fatigue Crack.

before the number of cycles n_i of stressing (the number of cycles excluding the period of stress range reduced to one half) reached 4×10^4 cycles. The beach mark 2 was formed during the second halving of the stress range and this fatigue crack was initiated at n_i after 4×10^4 cycles and before 8×10^4 cycles. Therefore, with this specimen fatigue cracks were produced at two locations on the weld metal bottom surface of the weld root which combined to become one crack during the second block stress repetition, which propagated to result in failure. It was immediately before failure that this fatigue crack appeared at the surface of the specimen.

With Specimen SB-41, one fatigue crack was formed from the weld metal bottom surface of the weld root. This specimen was subjected to a total of 14 stress blocks from which 11 beach marks were left on the fracture surface. Therefore, this fatigue crack was initiated during the third block. However, because the dimensions of the beach mark 1 are large and the space between 3 and 4 is wide compared with others, it could well be that 2 or 3 beach marks were overlooked, and it is surmised that in the case of this specimen also the fatigue crack was initiated

at an extremely early stage of repetitive stressing.

The fatigue crack of Specimen SB-43. similarly to the cases of the preceding two specimens, was initiated from the bottom surface of the weld metal of the weld root. The beach mark 1 was formed by the second halving of the stress range and it is clear that the fatigue crack was initiated prior to $n_i=4\times10^4$ cycles.

With Specimen SB-38, a fatigue crack was initiated from a machining flaw at the root face. This specimen was failured during the 23rd stress amplitude halving period and there were 13 beach marks left on the fracture surface. Accordingly, it is considered that this fatigue crack was initiated during the ninth block. Upon making observations in the same manner as under **3(3)**, it was found that the irregularities at the bottom surface of weld metal at places such as the stop and restart location were smaller than in other specimens, and it is thought this is the reason of fatigue crack initiation at such a location. Furthermore, this was the only specimen in which fatigue cracks could not be found at other than the fracture surface upon opening up the weld.

In the case of Specimen SB-40, the fillet portion was failured (Fracture Surface 1) at $n=$ 911120 cycles ($n_i=411120$), while later, upon continuing the testing, the parallel portion was failured (Fracture Surface 2) at $n=1624800$ cycles ($n_i=814800$). The size of the unfused

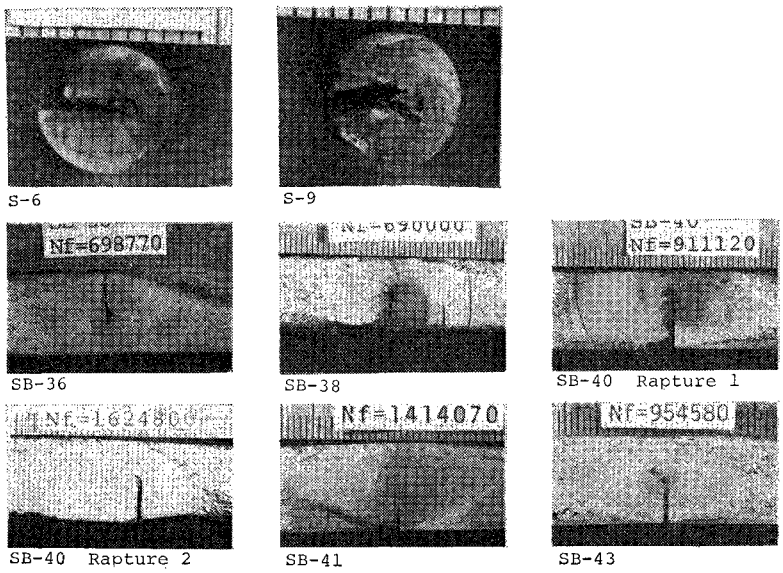

Photo 2 Fracture Surface with Beach Marks.

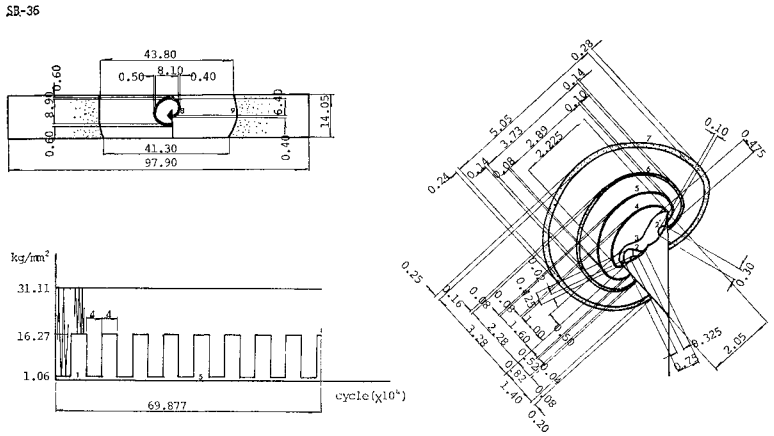

Fig. 4—(1)

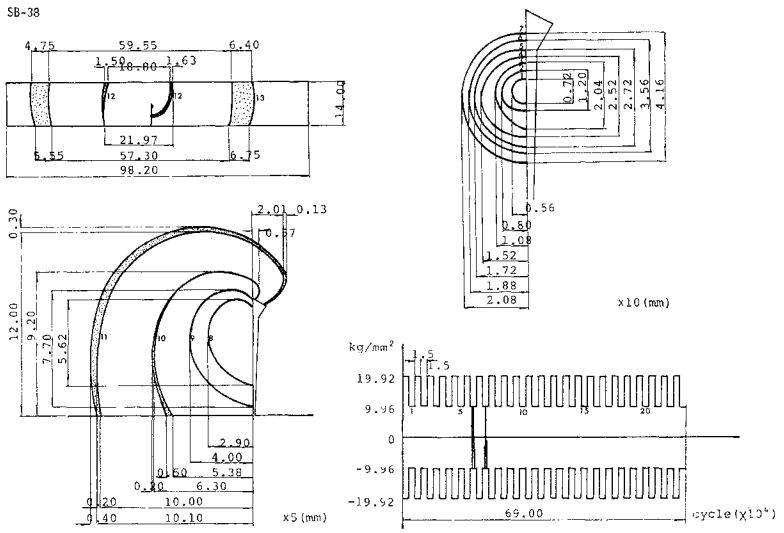

Fig. 4—(2)

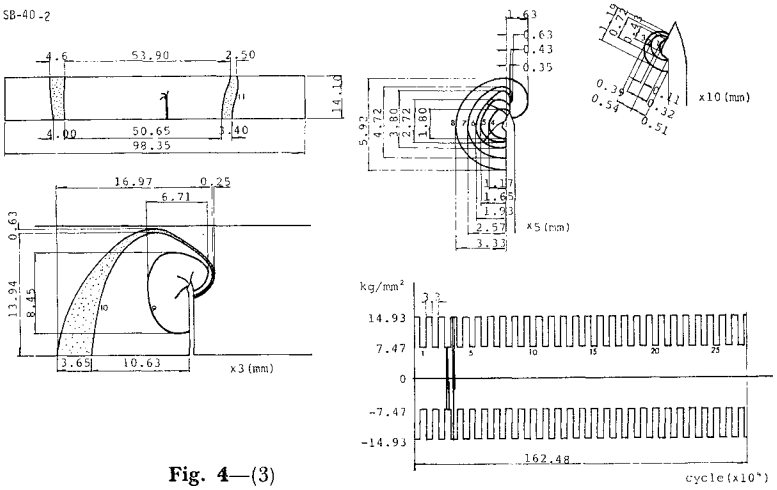

Fig. 4—(3)

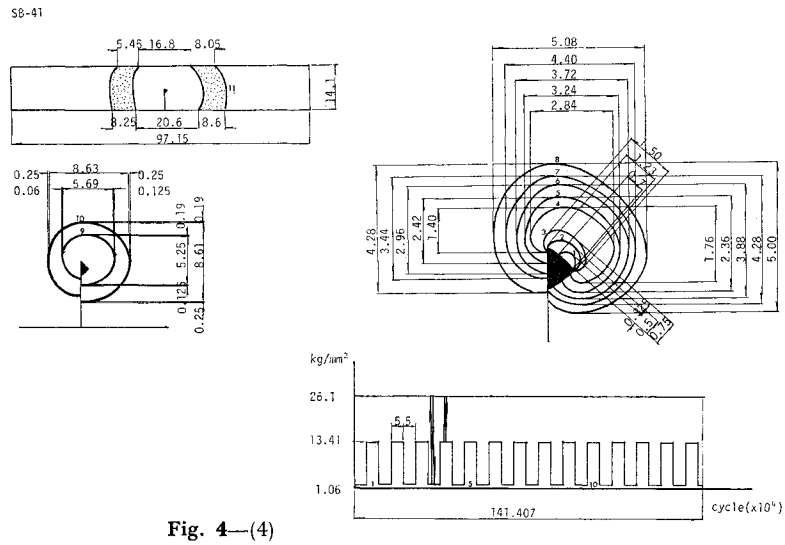

Fig. 4—(4)

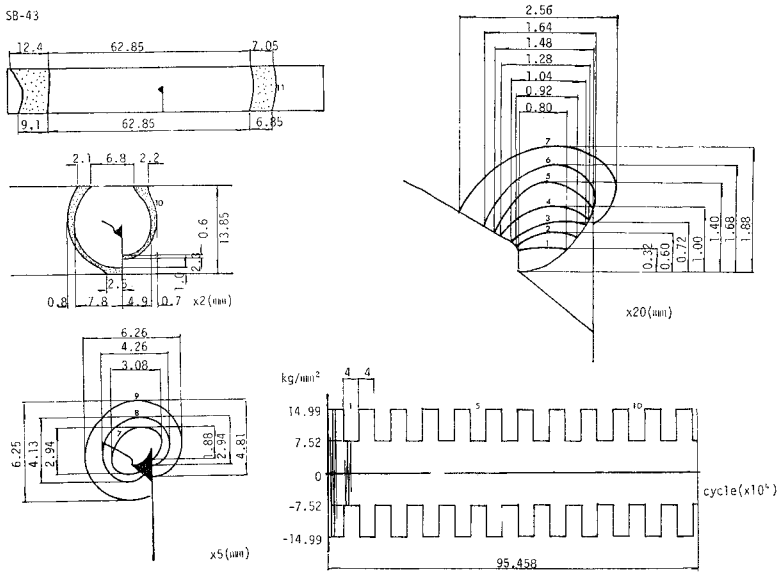

Fig. 4—(5)

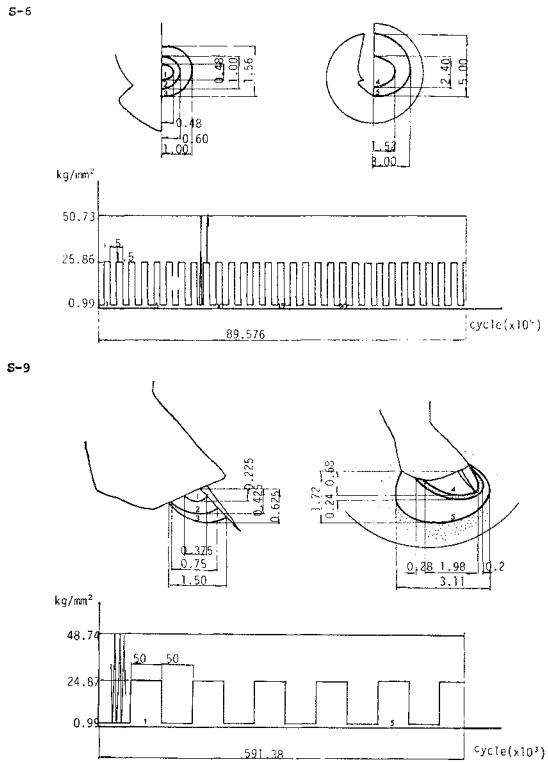

Fig. 4—(6)

Fig. 4—(1)～(6) Stress.

section of Fracture Surface 1 was considerably larger than that of Fracture Surface 2 (see **Photo 2**). On making observations similar to those of **Photo 1**, there was no very large unfused section at the parallel portion. At Fracture Surface 1 there was coincidence between the

number of times of stress range halving and the number of beach marks. In contrast, 11 beach marks were left on Fracture Surface 2, and it is thought the fatigue crack was initiated during the 16th block. From these test results and the test results of Specimen SB-38, it may be predicted that fatigue strength will be improved if welding is done in a manner to adequately melt the groove.

With Test Piece S-6, a fatigue crack was formed from the machined surface of the root face, and a fairly large number of stress repetitions was required until fatigue cracking similarly to the case of Specimen SB-38. In case of Test Piece S-9, fatigue cracking was initiated from the bottom surface of the weld metal at the unfused portion, and the number of beach marks was one less than the number of blocks. In **Photo 1**, the root gaps of Test Pieces S-6 and S-9 are considerably opened, these openings having been formed when the test pieces were failured.

Fig. 5 gives the results of beach mark tests with testing stress range indicated on the ordinate and number of cycles of stressing up to failure on the abscissa. The S-N_f curve obtained from constant stress range fatigue tests is also indicated in this figure. The results of the various beach mark tests are plotted roughly on the S-N_f curve, and it is clear that the influence on the life of halving stress ranges to form beach marks is of a degree that it can be ignored. The results of Specimens SB-38 and SB-4, and Test Piece S-6, which required a certain degree of repetitions of stressing until fatigue cracks were initiated, are located on the long life side of the S-N_f curve. Therefore, with most of the large-sized specimens and small-sized test pieces on which constant stress range tests were performed, it is surmised that fatigue cracks were initiated and began to propagate at extremely early stages of stress repetitions similarly to Specimens SB-36, SB-41 and SB-43, and Test Piece S-9.

(2) Propagation of Fatigue Crack

Here, as indicated in **Fig. 6**, fatigue cracks initiated from bottom surfaces of weld metal of unfused sections were classified as Type I until the fatigue crack length $2b$ became equal to weld metal bottom surface width w, with those past this point classified as Type II, and the crack depths a and crack lengths b of beach marks on the respective specimens were read. **Fig. 7** shows the results plotted taking crack depth a on the abscissa and crack length b on the ordinate, and according to this method of measuring crack dimensions, both Type I and Type II cracks have roughly $a=b$. Cases of fatigue cracks formed from root faces arranged in the manner of **Fig. 6** give similar results. From the fact that at a circular crack in an infinite plate subjected to tensile force the stress intensity factor along the circumference is constant, even if the crack configurations at the early stages are ununiform due to localized stress concentrations at locations of fatigue crack initiation, it is a predictable trend for cracks to be propagated in a manner to be circular.

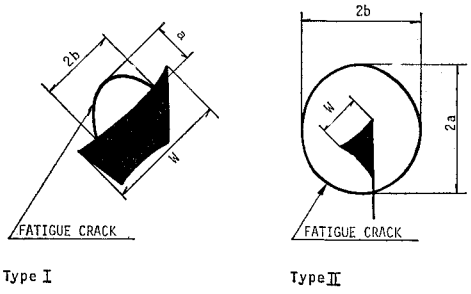

Fig. 6 Classification of Fatigue Crack and Size of It.

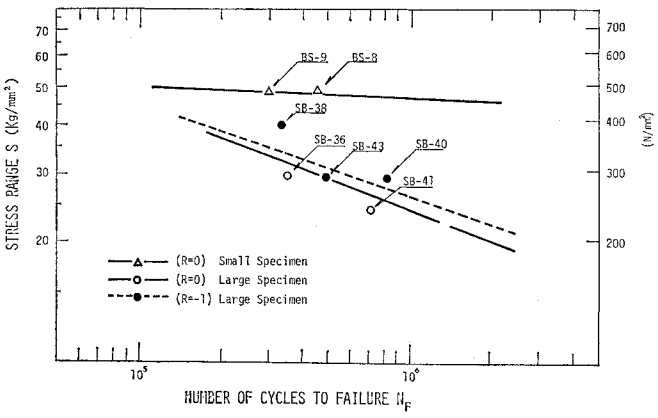

Fig. 5 Results of Beach Mark Tests.

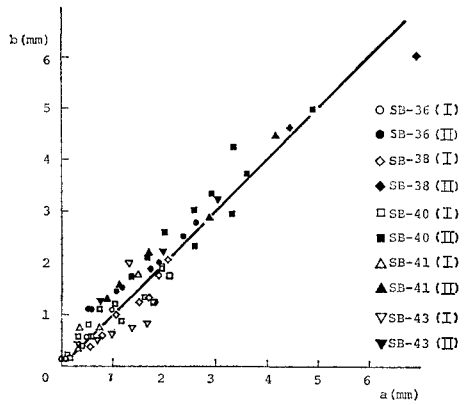

Fig. 7 Crack Depth a and Crack Length b.

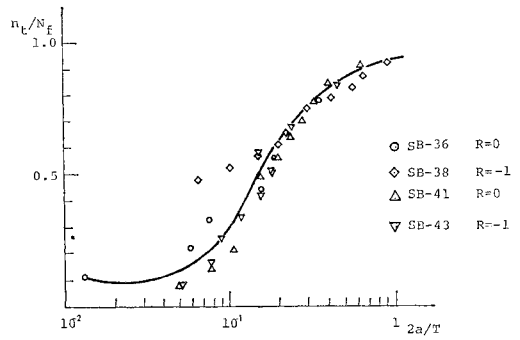

Fig. 8 Fatigue Crack Propagation from Bottom Surfaces of Welds.

Fig. 8 shows the dimensions $2a$ of beach marks of Specimens SB-36, -38, -41 and -43 in which fatigue cracks were initiated from bottom surfaces of welds at extremely early stages of load repetitions and the number of cycles (n_t) at which they were formed plotted with the abscissa (logarithm) as $2a/T$ (T: plate thickness) and ordinate as n_t/N_f. From this figure, the times at which fatigue cracks appear at the specimen surface ($2a/T=1$) are at 90% of the failure life elapsed or later, and therefore, in case of observing formation of a fatigue crack at the surface of a specimen, the life from appearance of the crack until failure will be very short. Further, it is clear that it will be at 80 to 90% of the failure life that the dimensions of a fatigue crack reaches about one half of the plate thickness ($2a \fallingdotseq 8$), while approximately 50% of the failure life is spent for the fatigue crack to propagate to diameter of about 3 mm.

In order to calculate the approximate stress intensity factor range (ΔK) of the fatigue cracks, it is thought acceptable to use the equation below with Type I cracks considered as semi-circular and Type II cracks as circular.

$$\Delta K=\frac{2}{\pi}S\sqrt{\pi a}\sqrt{\sec\left(\frac{\pi a}{T}\right)}$$

where

S: stress range
a: crack dimensions
T: plate thickness (circular)
1/2 of plate thickness (semi-circular)

In the above equation, $\sqrt{\sec(\pi a/T)}$ is a correction for finite plate thickness. However, in case of a semi-circular crack, ΔK calculated by the above equation is the value at Point B in **Fig. 6**.

Fig. 9 is the fatigue crack growth rate (da/dn) calculated from the spacings between beach marks plotted log-log for the stress intensity factor range ΔK at that time. The ΔK-da/dn relation obtained for steel of the same class as

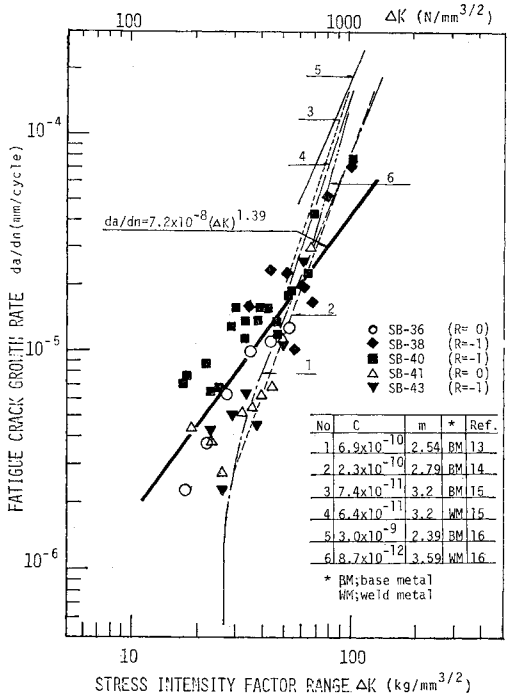

Fig. 9 Fatigue Crack Growth Rate from the Spacings between Beach Marks.

steel used in the tests here is indicated in the figure. The test values are fairly scattered, and it cannot be said that a linear relation (Paris Law)[12] holds true for the date of the each specimen, but as a whole a trend is indicated of the Paris Law being valid. The thick straight line in the diagram was obtained by the method of least squares. Several relations obtained by other studies[13)~16)] were also shown in the diagram. It is seen from the test values that there is a tendency for the fatigue crack growth rate to be faster than the existing ΔK-da/dn equation. This may be considered as the influence of residual tensile stress, and the causes may be said to be that the test values here are mainly of crack propagation at the weld metal, and that stress intensity factors are calculated with fatigue cracks of complex configurations considered as semi-circular or circular.

Of the test values given in Fig. 9, those for Specimens SB-36 and SB-41 were from fatigue tests with pulsating stresses ($R=0$), while the others were with alternating stresses ($R=-1$). However, in the ΔK-da/dn relationship of **Fig. 9**, differences due to these stress ratios are not perceptable. This also is an effect of residual welding stress. Therefore, the reason that the test results for $R=-1$ were for slightly longer life compared with the results for $R=0$ in **Fig. 2**

was considered to be that if of identical stress ranges, the maximum stress for $R=-1$ is one half of that for $R=0$, due to which the zone in which a fatigue crack can propagate is broadened (see **Fig. 4**).

5. CONCLUSIONS

Experimental studies were made of initiation and propagation properties of fatigue cracks in manually welded 45-degree single-bevel groove partial penetration longitudinal-bead joints, and the principal results obtained were the following:

(1) In all the specimens the penetration of weld metal into grooves was insufficient, and tunnel-like unfused portions remain over the entire lengths of the welds. Fatigue cracks are initiated from locations where configuration changes at bottom surfaces of welds. In almost all of the specimens, fatigue cracks were initiated from a plural number of places including stop and restart locations.

(2) In the greater part of the specimens subjected to beach mark tests, fatigue cracks were formed from bottom surfaces of weld metal at extremely early stages of the lives. Consequently, almost no length of life before initiation of fatigue cracking can be expected. At joints of good configurations of the bottom surfaces of weld metal, fatigue cracks were formed from machining defects of root faces, in which cases certain extents of stress repetitions were required until initiation of fatigue cracks.

(3) The relationship between testing stress range and the number of cycles required to failure in beach mark tests coincides roughly with the S-N_f curve obtained from constant stress range tests. Accordingly, it is surmised that in most of the specimens on which constant stress range fatigue tests were performed, fatigue cracks were initiated at extremely early stages of stress repetitions.

(4) Fatigue cracks produced at roots are propagated while becoming circular. With large-sized specimens, fatigue cracks appear at specimen surfaces on elapse of 90% or more of the failure life, and approximately 50% of the failure life is spent for the fatigue crack to propagate to diameter of about 3 mm.

(5) The relationship between stress intensity factor (ΔK) and fatigue crack propagation velocity (da/dn) obtained from the configurations and spacings of beach marks is close to the existing ΔK-da/dn relationship. The influence of stress ratio (R) on the ΔK-da/dn relationship is not recognized. These trends are all thought to be due to the influences of residual stresses.

(6) Constant stress range fatigue tests of large-sized specimens were performed at $R=0$ and $R=-1$, with the experimental results for the latter being for slightly longer life than for the former. Considering that the greater part of the life is for fatigue-crack propagation, and moreover, that there is no difference between propagation velocities, if in an identical stress range, the maximum stress for $R=-1$ is one half of that for $R=0$, and because of this the zone of stable propagation of fatigue cracks is broadened.

ACKNOWLEDGEMENTS

This studies were made with guidance and advice from Professor Toshio Nishimura of Tokyo Institute of Technology. The experimental work of the paper was performed by Technician Masayuki Tsurumaki of the Tokyo Institute of Technology and Research Associate Masaru Ueno of University of Tokyo. The authors wish to express their sincere gratitude to all those mentioned above.

REFERENCES

1) Japan Society of Civil Engineers: The Specifications of Steel Railway Bridges, 1974 (in Japanese).
2) Chang, Dong Il, C. Miki and T. Nishimura: Study on the Estimation of Fatigue Life of Steel Members by Linear Damage Rule, Proceedings of JSCE, No. 270, pp. 15~29, Feb. 1978 (in Japanese).
3) Forsyth: The Physical Basis of Metal Fatigue, Blackie and Son, p. 52, 1969.
4) Yamada, K., T. Makino and Y. Kikuchi: Fracture Mechanics Analysis of Fatigue Cracks Emanating from Toe of Fillet Weld, Proceedings of JSCE, No. 292, Dec. 1979 (in Japanese).
5) Frank, K. H. and J. W. Fisher: Fatigue Strength of Fillet Welded Cruciform Joints, Journal of the Structural Division, Proceedings of ASCE, Vol. 105, No. ST9, Sept. 1979.
6) Maddox, S. J. and D. Webber: Fatigue Crack Propagation in Aluminum-Zinc-Magnesium Alloy Fillet-Welded Joints, ASTM, STP. 648, pp. 159~184, 1978.
7) Maddox, S. J.: Assessing the Significance of Flaws in Welds Subject to Fatigue, Welding Journal, pp. 401s~409s, Sept. 1974.
8) Lawrence, F. V.: Estimation of Fatigue-Crack Propagation Life in Butt Welds, Welding Journal, pp. 2125~2325, May 1973.
9) Nishimura, T., J. Tajima, A. Okukawa and C. Miki: Fatigue Strength of Longitudinal Signle-Bevel-Groove Welded Joints, Journal of JSCE, No. 291, pp. 27~40, Oct. 1979 (in Japanese).

10) Japan Society of Civil Engineers: Fatigue Design for Honshu-Shikoku Bridges, pp. 147～150, 1974 (in Japanese).
11) Tajima, J., A. Okukawa, M. Sugizaki and H. Takenouchi: Fatigue Tests of Panel Point Structures of Truss Made of 80 kg/mm² High Tensile Strength Steel, IIW. Doc. No. XIII-831-77, July 1977.
12) Paris, D. C. and F. Erdogan: A Critical Analysis of Crack Propagation Laws, Transaction of the ASME, Journal of Basic Engineering, Series D, 85, No. 3, 1963.
13) Ohta, A., E. Sasaki and M. Kosuge: Effect of Stress Ratios on the Fatigue Crack Propagation Rate, Transactions of the JSME, Vol. 43, No. 373, pp. 3179～3191, Sept. 1977 (in Japanese).
14) Nishimura, T., M. Sakano, C. Miki: Evaluation of Fatigue Propagation Rate under Variable Stress Amplitude, Proc. of 34th Annual Meeting of JSCE, Sec. I, pp. 88～90, Oct. 1979 (in Japanese).
15) Narumoto, A., M. Tanaka, T. Funakoshi: Fatigue Crack Propagation of Various Structural Steels, Kawasaki Steels Technical Review, Vol. 6, No. 1, pp. 38～51, 1969-1 (in Japanese).
16) Ishihara, M., S. Hiraishi, T. Sugimoto: Fatigue Crack Growth Rate in Base Plate and Welded Joints of High Tensile Strength Steel, Journal of the Society of Materials Science, Japan, Vol. 27, No. 292, pp. 42～48, 1978-1 (in Japanese).

(Recieved April 14, 1980)